A passivity-based framework for stability analysis and control including power network dynamics

Chrysovalantis Spanias, Petros Aristidou, and Michalis Michaelides

***Abstract*—The ongoing efforts by many countries worldwide to increase the share of Renewable Energy Sources (RES) in power generation has changed the nature of existing power grids and introduced numerous stability-related issues. To address these problems, more extensive and detailed stability analysis studies are therefore needed. Driven by this need, in this paper, we present a passivity-based framework for stability analysis and control design that allows more accurate modelling of both the network and the power system components while facilitating the derivation of completely decentralized stability results. In particular, the proposed approach relies on the formulation of the network as a dynamical multi-variable system, which is shown to be passive, even when the network's dynamic and lossy nature are taken into account. The application of decentralized passivity conditions on bus dynamics is then further exploited, together with the incorporation of more accurate dynamical models for the power system components, to guarantee the asymptotic stability of the interconnected system. Moreover, we show the opportunities provided by the proposed approach through the design of a demand-side voltage droop controller and several dynamic simulations on two typical test systems.**

***Index Terms*—Network dynamics, power systems, passivity, stability analysis and control, multi-variable dynamical systems.**

I. Introduction

Over the last years, there is an ongoing, worldwide effort to decelerate climate change and global warming. This effort which focused on the reduction of greenhouse gas emissions, led countries to gradually replace the energy production from fossil-fueled plants with several "greener" power generation technologies [1]. As a result, the share of RES in power generation has significantly increased and is expected to reach 32% by the end of 2030 [2], [3]. Such a large share of RES, however, introduced new challenges that were not encountered in traditional power grids. In particular, the reduction of systems' rotational inertia along with the intermittent nature of RES made frequency and voltage deviations during disturbances steeper and the instability phenomena that occur more severe [4]–[6]. Moreover, the existing frequency and voltage control mechanisms are becoming too slow with respect to the disturbance dynamics and thus, unable to prevent or even effectively damp the occurring large frequency and voltage deviations.

C. Spanias, P. Aristidou and M. Michaelides are with the Department of Electrical Engineering, Computer Engineering and Informatics, Cyprus University of Technology, Limassol, Cyprus. e-mails: ca.spanias@edu.cut.ac.cy, petros.aristidou@cut.ac.cy, michalis.michaelides@cut.ac.cy.

Manuscript submitted April 27, 2020.

Aiming to overcome the above problems, more extensive power system stability studies are required. Such studies which take into account accurate dynamical models of both the network and the power system components, will not only assist in the design of more effective control mechanisms, but they will also provide useful information regarding the stability of the system. An important aspect that has to be considered, especially when stability is studied using decentralized conditions, is the consideration of the network's dynamic and lossy nature. Currently, the majority of the related literature adopts a static network formulation, using either active and reactive power flows, or the line current components [7]–[11]. For simplicity, networks are often considered lossless as well, which in turn affects the accuracy of the analysis and the validity of the derived stability results. Such examples can be found in [12]–[15]. Nevertheless, due to the lack of rotational inertia, the network's response becomes now comparable to the response of the rest of the system. Thus, the adoption of a static representation for power networks leads to more conservative stability results than those derived in the traditional stability analysis studies since the dynamic coupling between the bus dynamics with the grid becomes important, especially for the appropriate design of RES controllers.

Driven by the need for more accurate modelling within stability studies, in this paper, we introduce a passivity-based framework for stability analysis and control of existing low-inertia power systems wherein more accurate dynamical models of the network and the power system components are used. This paper extends and enhances the previous work in [16], with the following new contributions:

- The network model is formulated as a dynamical multi-variable system, and it is shown that it is passive, even when the network's dynamic and lossy nature are considered.
- More accurate dynamical models for the power system components are incorporated in the framework and more broad decentralized passivity conditions are imposed on bus dynamics to guarantee the asymptotic stability of the interconnected system.
- A methodology to design new, more effective, adaptive control mechanisms is proposed that is based only on local bus information. Such a decentralized control design can reduce the complexity of the analysis since it does not require the implicit knowledge of the system.

Subsequently, we assess the advantages and the opportunities offered by the proposed approach and demonstrate its applicability through the design of a voltage droop, load controller that can provide the necessary voltage support. Finally, we verify the significance of the adoption of such a multi-input/multi-output framework through several dynamic simulations on a simple test system and the IEEE 68 bus test system.

The rest of the paper is structured as follows: In Section II, we provide some basic preliminaries regarding network modelling. The proposed multi-variable framework is formulated in Section III. The main stability result derived when this framework is adopted, is presented in Section IV. Section V provides an assessment of the presented framework while its applicability is demonstrated through a design example of a load-side voltage control mechanism in Section VI. The significance of the proposed approach and the presented network formulation is verified in Section VII through dynamic simulations. Finally, conclusions are drawn in Section VIII.

II. Preliminaries

A power network with arbitrary topology can be described by a connected and undirected graph $(\mathcal{N}, \mathcal{E})$, where $\mathcal{N} = \{1, 2, \dots |\mathcal{N}|\}$ is the set of buses and $\mathcal{E} \subset \mathcal{N} \times \mathcal{N} = \{1, 2, \dots |\mathcal{E}|\}$ the set of lines connecting them. The network structure can be represented by its corresponding incidence matrix $E \in \mathbb{R}^{|\mathcal{N}|\times|\mathcal{E}|}$, similarly to [11]. By arbitrarily labeling the ends of the line l with a $+$ and a $-$, the matrix E is given by

$$E_{il} = \begin{cases} +1 & \text{if } i \text{ is the positive end of } l \\ -1 & \text{if } i \text{ is the negative end of } l \\ 0 & \text{otherwise.} \end{cases} \quad (1)$$

We also use $l = (i, j)$ to denote the link connecting the network buses i and j through the line l and $l \to i$ to denote that the line l is connected to bus i. For the formulation of a dynamical model to represent the network, we now make the following assumptions regarding the network lines and the system frequency.

Assumption 1: Network lines can be accurately represented by symmetric RLC elements (Π-equivalent).

Assumption 2: The network frequency ω, is almost constant at synchronous value ω_s (50 or 60 HZ), i.e. $\omega - \omega_s \approx 0$.

Assumption 1 states that any line can be represented by the traditional Π-equivalent similarly to the majority of the related literature [17]. Moreover, in Assumption 2, we consider that the variations of the network frequency are very small which is also a mild assumption considering that the maximum frequency deviation in the European Network of Transmission System Operators for Electricity (ENTSO-E) system is $200mHz$ ($\pm 0.4\%$) [18].

We also introduce here the diagonal matrices R, L and $C \in \mathbb{R}^{|\mathcal{E}|\times|\mathcal{E}|}$ which contain the resistance, the inductance and the capacitance of each line across the network. We get:

$$R_{ml} = \begin{cases} R_l & \text{if } m = l \\ 0 & \text{otherwise} \end{cases} \quad (2)$$

$$L_{ml} = \begin{cases} L_l & \text{if } m = l \\ 0 & \text{otherwise} \end{cases} \quad (3)$$

and

$$C_{ml} = \begin{cases} C_l & \text{if } m = l \\ 0 & \text{otherwise} \end{cases} \quad (4)$$

where R_l,L_l and C_l denote the resistance, the inductance and the capacitance of the line l respectively. We note that C_l could be considered equal to zero when l corresponds to a Low Voltage (LV) distribution line of the system.

III. Framework formulation

A. Network Dynamics

For the derivation of a multi-variable network representation, we introduce the differential equations describing the current components at the series impedances and the voltage components at the shunt capacitances of each line $l \in \mathcal{E}$ of the network. Using the network's incidence matrix we then define the net injected current components at every bus $i \in \mathcal{N}$ across the grid. These equations are subsequently employed in formulating the proposed dynamical network representation which is depicted in Fig. 1. As it can be observed, the power network constitutes a multi-input/multi-output system originating from the negative feedback connection of the branch and capacitance dynamics. It should be also noted that all variables/states of the proposed network model are expressed on a *common system reference frame*, i.e. two common axes that rotate at a specific velocity ω [17].

Firstly, we define the phasors of the current of line $l \in \mathcal{E}$ and the voltage of bus $i \in \mathcal{N}$ in their rectangular form as follows:

$$\hat{I}_l = I_{a,l} + jI_{b,l} \text{ and } \hat{V}_i = V_{a,i} + jV_{b,i} \quad (5)$$

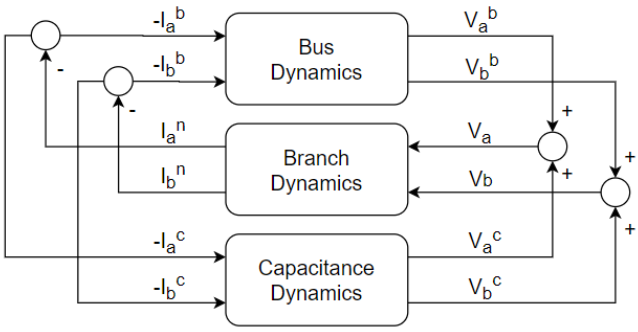

Fig. 1. The power network represented as an interconnection of input/output systems associated with the bus and network dynamics, respectively [16].

where $I_{a,l}$ and $I_{b,l}$ are the current components of line l and $V_{a,i}$ and $V_{b,i}$ are the voltage components of bus i. Based on the phasor representation provided in [19], the state equations of the line current of line l are given by:

$$L_l\dot{I}_{a,l} = -R_l I_{a,l} - \omega L_l I_{b,l} + (V_{a,i} - V_{a,j}) \quad (6)$$

$$L_l\dot{I}_{b,l} = -R_l I_{b,l} + \omega L_l I_{a,l} + (V_{b,i} - V_{b,j}) \quad (7)$$

where $V_{a,i}$, $V_{b,i}$, $V_{a,j}$ and $V_{b,j}$ are the voltage components at buses i and j which are connected through line l. Considering that Assumption 2 holds, the differential equations can be further simplified as follows:

$$L_l\dot{I}_{a,l} = -R_l I_{a,l} - \omega_s L_l I_{b,l} + (V_{a,i} - V_{a,j}) \quad (8)$$

$$L_l\dot{I}_{b,l} = -R_l I_{b,l} + \omega_s L_l I_{a,l} + (V_{b,i} - V_{b,j}). \quad (9)$$

We now define the net injected current components at each bus of the grid by employing the incidence matrix E. The net injected current components at bus i are therefore given by the following set of equations:

$$I^n_{a,i} = \sum_{l=1}^{|\mathcal{E}|} E_{il} I_{a,l} \text{ and } I^n_{b,i} = \sum_{l=1}^{|\mathcal{E}|} E_{il} I_{b,l} \quad (10)$$

which are the Kirchoff's Current Law equations at each bus of the grid. By introducing the vectors $I_a = [I_{a,1} I_{a,2} \dots I_{a,|\mathcal{E}|}]^T$, $I_b = [I_{b,1} I_{b,2} \dots I_{b,|\mathcal{E}|}]^T$, $I^n_a = [I^n_{a,1} I^n_{a,2} \dots I^n_{a,|\mathcal{N}|}]^T$, $I^n_b = [I^n_{b,1} I^n_{b,2} \dots I^n_{b,|\mathcal{N}|}]^T$, $V_a = [V_{a,1} V_{a,2} \dots V_{a,|\mathcal{N}|}]^T$ and $V_b = [V_{b,1} V_{b,2} \dots V_{b,|\mathcal{N}|}]^T$, the branch dynamics can be represented by the following dynamical system with inputs the vectors of bus voltage components V_a and V_b, states the vectors of line current components I_a and I_b, and outputs the vectors of net injected current components I^n_a and I^n_b:

$$\begin{bmatrix} \dot{I}_a \\ \dot{I}_b \end{bmatrix} = \begin{bmatrix} K_A & \omega_s I^{\mathcal{E}} \\ -\omega_s I^{\mathcal{E}} & K_A \end{bmatrix} \begin{bmatrix} I_a \\ I_b \end{bmatrix} + \begin{bmatrix} K_B & 0 \\ 0 & K_B \end{bmatrix} \begin{bmatrix} V_a \\ V_b \end{bmatrix} \quad (11)$$

$$\begin{bmatrix} I^n_a \\ I^n_b \end{bmatrix} = \begin{bmatrix} K_C & 0 \\ 0 & K_C \end{bmatrix} \begin{bmatrix} I_a \\ I_b \end{bmatrix} \quad (12)$$

The matrices $K_A \in \mathbb{R}^{|\mathcal{E}|\times|\mathcal{E}|}$, $K_B \in \mathbb{R}^{|\mathcal{E}|\times|\mathcal{N}|}$ and $K_C \in \mathbb{R}^{|\mathcal{N}|\times|\mathcal{E}|}$ can be deduced from the set of differential equations (8)-(10) as follows:

$$K_A = -L^{-1}R \quad (13)$$

$$K_B = L^{-1}E^T \quad (14)$$

and

$$K_C = E \quad (15)$$

where $I^{\mathcal{E}}$ is the $\mathbb{R}^{|\mathcal{E}|\times|\mathcal{E}|}$ identity matrix.

On the other hand, capacitance dynamics are derived using the following state equations of the voltage components at the shunt capacitance of line $l \to i$:

$$\frac{C_{l\to i}}{2}\dot{V}^c_{a,i} = \omega_s \frac{C_{l\to i}}{2} V^c_{b,i} - I^c_{a,i} \quad (16)$$

$$\frac{C_{l\to i}}{2}\dot{V}^c_{b,i} = -\omega_s \frac{C_{l\to i}}{2} V^c_{a,i} - I^c_{b,i} \quad (17)$$

where $I^c_{a,i}$ and $I^c_{b,i}$ are the components of the current absorbed by the shunt capacitance $C_{l\to i}$ at bus i. Using the differential equations (16) - (17), capacitance dynamics can be now expressed in the following compact matrix form:

$$\begin{bmatrix} \dot{V}^c_a \\ \dot{V}^c_b \end{bmatrix} = \begin{bmatrix} 0 & \omega_s I^{\mathcal{N}} \\ -\omega_s I^{\mathcal{N}} & 0 \end{bmatrix} \begin{bmatrix} V^c_a \\ V^c_b \end{bmatrix} - \begin{bmatrix} \mathcal{C}^{-1} & 0 \\ 0 & \mathcal{C}^{-1} \end{bmatrix} \begin{bmatrix} I^c_a \\ I^c_b \end{bmatrix} \quad (18)$$

V^c_a, V^c_b, I^c_a and I^c_b denote the vectors of voltage and absorbed current components at the shunt capacitances connected to every bus $i = 1, 2, \dots, |\mathcal{N}|$ of the network, respectively. Furthermore, the matrix $I^{\mathcal{N}} \in \mathbf{R}^{\mathcal{N}\times\mathcal{N}}$ is the corresponding identity matrix while $\mathcal{C}$ can be deduced from equations (16) - (17) as follows:

$$\mathcal{C} = \frac{1}{2} E C E^T I^{\mathcal{N}}. \quad (19)$$

B. Passivity of network dynamics

We now examine the passivity properties that are revealed for the network through the adoption of such a dynamical multi-variable formulation. However, before doing so, we first provide the following fundamental passivity definition [20].

Definition 1: Consider the following dynamical system with inputs $u \in \mathbb{R}^p$, states $x \in \mathbb{R}^n$ and outputs $y \in \mathbb{R}^p$

$$\dot{x} = f(x, u) \quad (20)$$

$$y = h(x, u) \quad (21)$$

where $f : \mathbb{R}^n \times \mathbb{R}^p \to \mathbb{R}^n$ is locally Lipschitz, $h : \mathbb{R}^n \times \mathbb{R}^p \to \mathbb{R}^p$ is continuous, $f(0, 0) = 0$, and $h(0, 0) = 0$. The system (20) - (21) is passive if there exists a continuously differentiable positive semidefinite function $\mathcal{V}(x)$ (called the storage function) such that the following inequality holds:

$$u^T y \geq \dot{\mathcal{V}}(x), \ \forall (x, u) \in \mathbb{R}^n \times \mathbb{R}^p. \quad (22)$$

Moreover, if $u^T y = \dot{\mathcal{V}}(x)$ the system (20) - (21) is said to be lossless.

Lemma 1: The branch dynamics defined in (11)-(12) with inputs the vectors of bus voltage components V_a and V_b, states the vectors of line current components I_a and I_b, and outputs the vectors of net injected current components I^n_a and I^n_b constitute a passive $2|\mathcal{N}|$-input$\times 2|\mathcal{N}|$-output system.

Lemma 2: The capacitance dynamics defined in (18) with inputs the vectors of current components $-I^c_a$ and $-I^c_b$ and states/outputs the vectors of voltage components V^c_a and V^c_b constitute a lossless $2|\mathcal{N}|$-input$\times 2|\mathcal{N}|$-output system.

Remark 1: The passivity of any power network with arbitrary topology can be also shown through the use of the Positive-real Lemma for LTI systems [20]–[22]. Particularly, the Positive-real lemma which is the representation of Kalman-Yakubovich-Popov (KYP) condition using a LMI, states that a stable Linear Time Invariant (LTI) system[1] with

[1]The branch dynamics (11) - (12) constitute a stable stable system since the state matrix is negative definite and thus its eigenvalues lie in the left half of the complex plane.

minimal state representation $\Sigma = \{A, B, C, D\}$ is passive if and only if there exists a positive definite matrix P such that the following inequality holds:

$$\begin{bmatrix} A^T P + PA & PB - C^T \\ B^T P - C & -D - D^T \end{bmatrix} < 0. \quad (23)$$

The above inequality was verified for branch dynamics in [23] through a numerical application on the Kundur's Four-Machine Two-Area test system by considering that matrix $P^n = P^{nT} \in \mathbb{R}^{2|\mathcal{E}|\times 2|\mathcal{E}|}$ is given by:

$$P^n = \begin{bmatrix} L & 0 \\ 0 & L \end{bmatrix} \quad (24)$$

Remark 2: A similar network representation that takes into account the network's dynamic behavior and leads to identical results as those presented in Lemmas 1 - 2, is provided in [24]. The difference between the two dynamical formulations lies in the fact that the network system in [24] has inputs the vectors of net injected current components and outputs the vectors of the bus voltages, i.e. $u^T = [I_a^{nT}\ I_b^{nT}]$ and $y^T = [V_a^T\ V_b^T]$.

C. Multi-variable formulation of bus dynamics

The incorporation of bus dynamics into the proposed multi-variable framework can be carried out similarly as in [16]. Particularly, the bus models are expressed in a common system reference frame instead of their local dq-coordinates by incorporating Park-Clarke transformation into bus dynamics. Additionally, we consider that each power system component constitutes a device that either produces or consumes power in normal operating conditions and can be attached to a single bus (e.g. synchronous machines, motors, wind turbines, etc.) or two buses (e.g.HVDC lines, AC/DC converters, etc.). As presented in [25], the power system components can be represented as voltage sources that either inject or absorb current in the network and hereon, they will be referred to as *injectors*. Specifically, the components that are connected to a single bus will be denoted as *single-bus injectors* while for the components that are connected to two buses we will use the term *double-bus injector*. The proposed configuration can be visualized in Fig. 2.

Subsequently, to fit with the network formulation described in the previous sections, we consider that each single-bus injector forms a 2-input×2-output system while double-bus injectors are modelled by a 4-input×4-output system. Each injector is connected to the network (branch and capacitance) dynamics as illustrated in Fig. 1. For the representation of either the single-bus or the double-bus injectors, we now employ the broad class of dynamical systems (20)-(21). The vectors u, x and y denote the inputs, the states and the outputs of the system respectively. The dimensions of the vectors u and y depend on the type of the component, that is a single-bus or a double-bus injector. In particular, a single-bus injector at bus i has inputs the phasor components of the net injected currents $u = (-I_{a,i}^b,\ -I_{b,i}^b) \in \mathbb{R}^2$ and outputs the phasor components of the bus voltages $y = (V_{a,i}^b,\ V_{b,i}^b) \in \mathbb{R}^2$. On the other hand, a double-bus injector which is attached to buses i and j, has inputs the phasor components of the net injected currents at buses i and j, i.e. $u = (-I_{a,i}^b,\ -I_{a,j}^b,\ -I_{b,i}^b,\ -I_{b,j}^b) \in \mathbb{R}^4$ and outputs the phasor components of the bus voltages at buses i and j, i.e. $y = (V_{a,i}^b,\ V_{a,j}^b,\ V_{b,i}^b,\ V_{b,j}^b) \in \mathbb{R}^4$. The states $x \in X \subset \mathbb{R}^n$ of the dynamical system (20) - (21) are of arbitrary dimension since they are directly related to the dynamical model that is employed to represent the component.

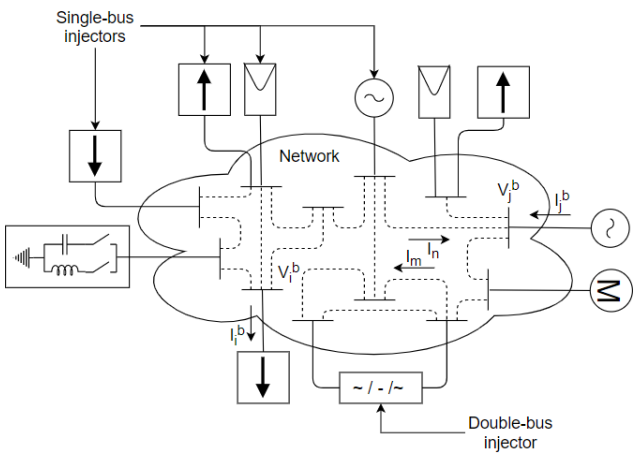

Fig. 2. An overview of the proposed power system configuration.

D. Necessary conditions for the asymptotic stability of the interconnected system

The natural passivity properties that were revealed for the network along with the proposed system structure[2] allows us to deduce significant stability results for the interconnected system by only imposing several local passivity conditions on bus dynamics. However, before presenting these conditions, it is necessary to provide here the following definitions regarding the equilibria of an interconnected system and the property of strict passivity.

Definition 2: The constant vector $[\hat{x}^T\ \hat{I}_a^T\ \hat{I}_b^T\ \hat{V}_a^{cT}\ \hat{V}_b^{cT}] \in \mathbb{R}^{(n+2|\mathcal{E}|+2|\mathcal{N}|)}$ is an equilibrium of the interconnected system (20) - (21), (11) - (12) and (18), if the time derivative of the states in (20), the line currents in (11) and the shunt capacitance voltages (18) are equal to zero.

Definition 3: Let the system (20)-(21) of Definition 1 and its equilibrium $(\hat{x}, \hat{u}) \in X \times U$, where $X \subset \mathbb{R}^n$ and $U \subset \mathbb{R}^p$. The system (20)-(21) is locally strictly passive if there exists a continuously differentiable function $\mathcal{V}$ (called the storage function) such that

$$(u - \hat{u})^T (y - \hat{y}) \geq \dot{\mathcal{V}} + \psi(x - \hat{x}),\ \forall (x, u) \in X \times U \quad (25)$$

[2]The power system is represented by the negative feedback interconnection of multiple subsystems, i.e. the branch, the capacitance and the bus dynamics.

for some positive definite function $\psi(x-\hat{x})$. Additionally the above system is:

- locally input strictly passive if $(u-\hat{u})^T(y-\hat{y}) \geq \dot{\mathcal{V}} + \phi(u-\hat{u})$ for some positive definite ϕ, $\forall u \neq \hat{u}$
- locally output strictly passive if $(u-\hat{u})^T(y-\hat{y}) \geq \dot{\mathcal{V}} + \rho(y-\hat{y})$ for some positive definite ρ, $\forall y \neq \hat{y}$.

In both the above cases, the inequalities should hold for all $(x,u) \in X \times U$.

Assumption 3: For each $i,\ j \in \mathcal{N}$, each of the bus dynamical systems (20)-(21) satisfies any of the local passivity properties about $[\hat{x}^T\ \hat{I}_a^{bT}\ \hat{I}_b^{bT}]$, in the sense described in Definitions 1 - 2.

As in [13] and [16], we assume that the aforementioned passivity properties hold without specifying the precise form of the bus dynamics. This allows us to incorporate into the stability analysis various power system components such as synchronous generators, inverter-based RES, loads, Flexible Alternating Current Transmission System (FACTS), High Voltage Direct Current (HVDC) lines etc. Additionally, more accurate, higher-order bus dynamical models along with their voltage and frequency regulation mechanisms can be also considered. Finally, to guarantee asymptotic convergence to the equilibria, we will require an additional condition related to the behaviour of the bus dynamics. This condition which will be used within the proof of Theorem 1, is a technical condition often satisfied[3].

Assumption 4: The storage functions $\mathcal{V}_i$ in Assumption 3 have a strict local minimum at the point $\hat{x}_i$.

IV. Main stability result

In this section, we state our main stability result when the proposed multi-input/multi-output stability analysis framework is adopted. This result which is independent of the network topology can provide decentralized guarantees for the asymptotic stability of any power system requiring only the local passivity conditions of Assumptions 3 - 4 to be satisfied by bus dynamics. Moreover, it is highlighted that these stability guarantees are derived without neglecting the dynamic and lossy nature of the lines.

Theorem 1: Suppose there exists an equilibrium of the interconnected system (20) - (21), (11) - (12) and (18) for which the bus dynamics (20) - (21) satisfy[4] Assumptions 3 - 4 for all $i,\ j \in \mathcal{N}$. Then this equilibrium is asymptotically stable, i.e. there exists an open neighbourhood S about this point such that for all initial conditions $[\hat{x}(0)^T\ \hat{I}_a(0)^T\ \hat{I}_b(0)^T\ \hat{V}_a^c(0)^T\ \hat{V}_b^c(0)^T] \in S$, the solutions of the system converge to this point.

Remark 3: The above stability result is completely decentralized and identical to the one presented in [16]. However, in this paper, along with the dynamic nature of the network, we considered that more broad passivity conditions are imposed on bus dynamics to guarantee the asymptotic convergence to the equilibrium. In particular, apart from an input-strict passivity condition on bus dynamics, we showed that asymptotic stability can be also deduced through output-strict and/or strict passive systems. Moreover, when the storage function of a power system component is positive definite, even a simple passivity condition can be sufficient to show that the interconnected system is local asymptotically stable. This will be shown in Section VI through the design of an alternative voltage droop load controller.

[3]The storage function of any observable and controllable linear system has a local minimum at its equilibrium.

[4]Bus dynamics shall satisfy at least one of the local conditions presented in Assumption 3.

V. Assessment of the proposed framework

The multi-variable dynamical formulation adopted in this paper is based on the approach presented in [16] and [26] where the analysis was carried out in a *common system reference frame*, instead of each bus local dq reference frame. The use of this system reference frame approach allows us to capture the natural passivity properties of the network which are then used for the derivation of completely decentralized stability results for the interconnected system. It should be mentioned that the passivity of the network is revealed without resorting to significant simplifications such as the consideration of lossless and static lines. Such simplifications are usually necessary when the analysis is carried out using the local dq coordinates due to the different bus frequencies and the voltage angles that are appearing in the network equations [24].

Throughout this work, we additionally take into account the network's dynamic behaviour. Such a network representation becomes crucial since the dynamic interaction of inverter-based DER with the rest of the system constitutes an important aspect in the analysis of the future power grids where RES share in power generation will dominate. Particularly, the dynamics of inverter-based DER are on similar time scales as the line dynamics while their controls are also significantly faster than synchronous generators' control mechanisms [5]. Moreover, as shown in [19], the dynamic coupling between inverter-based DER and the network is in many cases unstable although the capability of DER to employ fast-acting control mechanisms may lead to the expectation for more efficient frequency and voltage support.

Additionally, the flexibility provided regarding the accurate modelling of a variety of power system components constitutes another significant advantage of the proposed framework. In particular, when stability is deduced by in a completely decentralized manner, the elaborated analysis becomes more complex and thus difficult to incorporate higher-order dynamical models. This often coerces scientists to resort to simpler models that even if they can facilitate the analysis, they cannot ensure the reliability of the derived results.

Finally, the proposed passivity-based framework can also drive the appropriate selection/tuning of the grid-connected components which are often non-passive. Specifically, the local passivity conditions presented in Section III can assist

in the design of more accurate distributed voltage and frequency control mechanisms or the improvement of existing controllers. At the same time, they can significantly reduce the complexity of the analysis since are sufficient for ensuring the overall system stability and robustness without requiring the explicit knowledge of the network structure. Examples of the application of such passivity-based techniques can be found in [13], [16], [24].

VI. Example: A load-side voltage droop controller

A. Controller design

To help the reader understand the applicability of the proposed approach, we present here the design of an alternative, demand-side voltage droop controller, This control mechanism was initially introduced in [27] to provide the necessary voltage support to the distribution grid. In particular, we consider that all loads are represented by a constant impedance model as follows:

$$\begin{bmatrix} V_{a,i}^b \\ V_{b,i}^b \end{bmatrix} = \begin{bmatrix} R_i^L & -X_i^L \\ X_i^L & R_i^L \end{bmatrix} \begin{bmatrix} -I_{a,i}^l \\ -I_{b,i}^l \end{bmatrix} \tag{26}$$

where R_i^L and X_i^L denote the resistance and the impedance of the load[5] connected at bus i respectively. We also consider that a part of these loads is controllable and thus can participate in system operation. We thus introduce a negative feedback control mechanism that can regulate voltage through the control of the current absorbed by these loads. The proposed mechanism can be illustrated in Fig. 3 and is described by the following set of differential equations:

$$\begin{bmatrix} \dot{I}_{a,i}^{cl} \\ \dot{I}_{b,i}^{cl} \end{bmatrix} = A_i^c \begin{bmatrix} I_{a,i}^{cl} \\ I_{b,i}^{cl} \end{bmatrix} + B_i^c \begin{bmatrix} V_{a,i}^b - V_{a,i}^{ref} \\ V_{b,i}^b - V_{b,i}^{ref} \end{bmatrix}. \tag{27}$$

$I_{a,i}^{cl}$ and $I_{b,i}^{cl}$, and $V_{a,i}^{ref}$ and $V_{b,i}^{ref}$ denote the phasor components of the mechanism's output current and the reference voltage at bus i respectively. The matrices A_i^c, $B_i^c \in \mathbb{R}^{2\times 2}$ in (27) are given as follows:

$$A_i^c = \frac{1}{T_{c,i}} \begin{bmatrix} -1 & 0 \\ 0 & -1 \end{bmatrix} \quad \text{and} \quad B_i^c = \frac{1}{T_{c,i}} \begin{bmatrix} k_{a,i}^c & k_{b,i}^c \\ -k_{b,i}^c & k_{a,i}^c \end{bmatrix}$$

where $k_{a,i}^c$, $k_{b,i}^c \geq 0$ are the gain constants and $T_{c,i}$ is the time constant of the controller.

Remark 4: All variables within load dynamics (26) and (27) are expressed in a common reference frame as described in Section III. Moreover, the reference inputs $V_{a,i}^{ref}$ and $V_{b,i}^{ref}$ are derived through the Park-Clarke transformation of a voltage reference setpoint V_i^{ref} using the same angle difference δ_i.

[5]The negative sign in (26) appears due to the fact that $I_{a,i}^l$ and $I_{b,i}^l$ denote here the components of the net absorbed current rather than the net injected current.

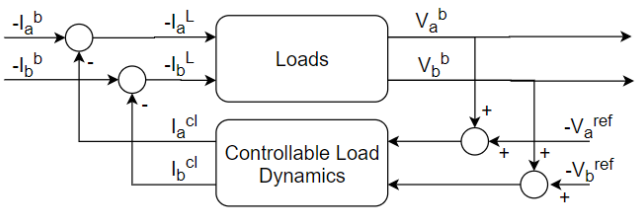

Fig. 3. The load-side voltage controller connected in a negative feedback arrangement to bus/load dynamics.

B. Passivity of load dynamics

To guarantee the asymptotic stability of the interconnected system presented in Fig. 1, the controllable load dynamics (26) and (27) and the rest of the power system components must satisfy one of the local passivity conditions presented in Definitions 1 - 2. We, therefore, provide the following proposition wherein we show that the controllable load dynamics are passive and thus can assist in power system operation during disturbances.

Proposition 1: The controllable load dynamics (26) and (27) constitute a 2-input $\times$ 2-output passive system.

Remark 5: An important advantage of this voltage droop controller lies in the fact that it can be employed in either centralized or decentralized fashion. Particularly, the voltage setpoints can be defined locally at the loads (e.g. thermal loads controlled by power electronics) or can be received from a SCADA/DMS during voltage dips or rises.

Remark 6: As we are about to show in Section VII, although we do not require all power system components to satisfy any of the aforementioned passivity conditions, the employment of the presented voltage droop controller on several loads can significantly improve the response of the system during disturbances. This relies on the fact that additional damping is provided to the grid through the utilization of the proposed control scheme.

VII. Simulations

In this section, we verify the significance of our stability analysis framework through several dynamic simulations on the two typical test systems that are presented in Figs. 4 and 5 respectively. In particular, we first examine the dynamic response of the system during a disturbance when the proposed dynamical network model is adopted. The investigation is carried out on the simple four area test system that is illustrated in Fig. 4. This test system consists of four areas that are connected through a typical $230kV$ transmission line of various lengths and of the following characteristics: $r = 0.0001pu/km$, $x = 0.001pu/km$ and $b = 0.00175pu/km$ ($S_b = 100MVA$). For the representation of all areas, we use the classical third-order synchronous generator model and the ZIP load model [17], [20]. Both models can be written in the form (20) - (21) and consequently can be easily incorporated into the stability analysis using the proposed framework.

To show the effect of such a dynamic network modelling, we consider a sudden increase of $100MW$ of load at area 2 under the following three power system conditions: (a) low RES penetration, (b) medium RES penetration and (c) high RES penetration. These conditions were achieved by increasing the RES penetration as a constant PQ injection at the four buses. At the same time, we decreased the synchronous generator output which in turn yields in a significant reduction of system's inertia. The results of these simulations are illustrated in Figures 6 - 11 through the representation of the voltage and the frequency response at area 2 when either a lossless, a static and a dynamic network model are adopted. As we observe from the figures, the use of a lossless network model results in a less accurate voltage and frequency response since although the line resistance is significantly smaller than its inductance, it still affects the voltage and the frequency across the grid. On the other hand, both the static and dynamic network representation result in a quite similar response. However, while the RES penetration increases, considerable low-frequency oscillations are appearing when a dynamic network model is used. These voltage and frequency oscillations are becoming larger and faster as both the line's length and the RES penetration increase. This directly leads to the conclusion that as RES share in power generation increases, more accurate dynamical models are necessary to ensure the reliability and the robustness of the system.

The effectiveness of the presented passivity-based framework to guarantee system stability in a completely decentralized manner and design new distributed control schemes is presented through several dynamic simulations on the IEEE 68 bus test system [28]. For these simulations, we also consider that a sudden load change of 100MW occurs at buses 1, 7, 21, 28 and 46 while loads at buses 3, 4, 16, 24, 26, 33, 40, 47, 49 and 50 are equipped with the proposed voltage control mechanism. The gain and the time constants of the controller are set at all controllers as follows: $K_a = 5pu$, $K_b = 1pu$ and $T_c = 0.1sec$. The effect of the proposed controller is illustrated in Figs. 12 - 13 by the voltage and the frequency deviation at bus 32 when Power System Stabilizers

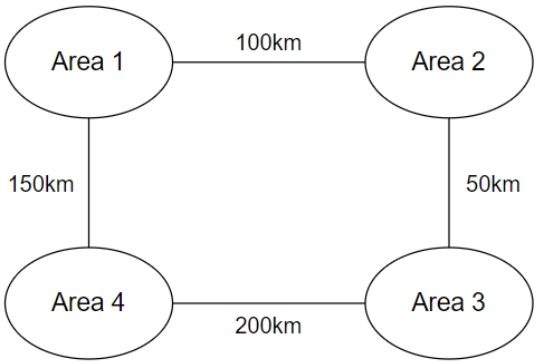

Fig. 4. Single line diagram of a simple four area test system.

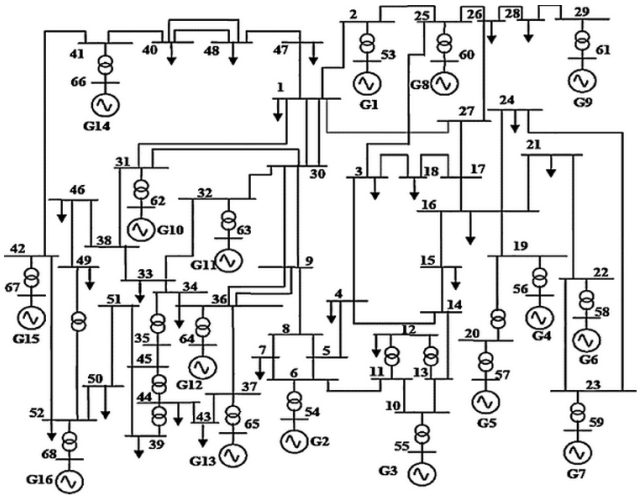

Fig. 5. Single line diagram of the IEEE 68-bus test system (New York / New England).

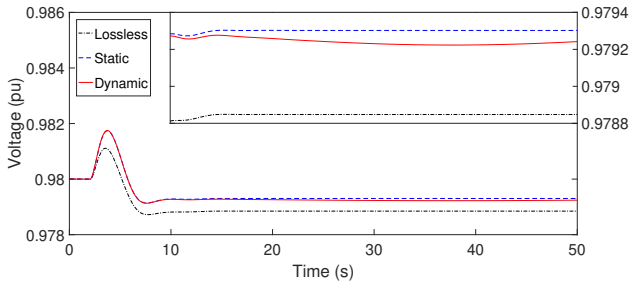

Fig. 6. The voltage deviation at area 2 under low RES penetration conditions.

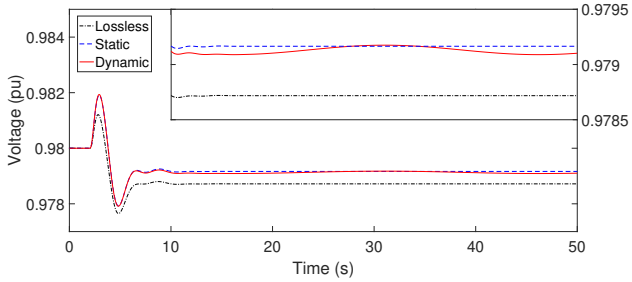

Fig. 7. The voltage deviation at area 2 under medium RES penetration conditions.

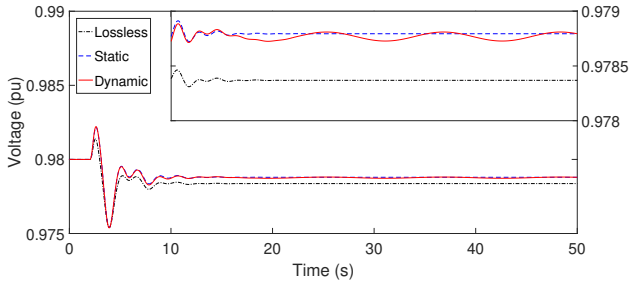

Fig. 8. The voltage deviation at area 2 under high RES penetration conditions.

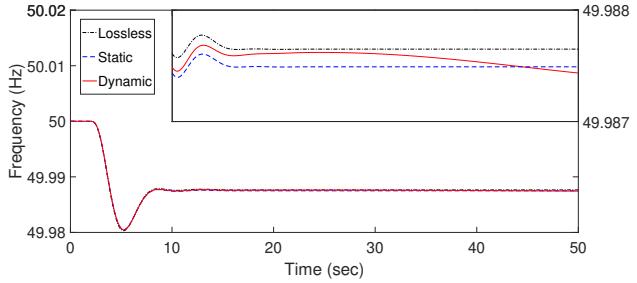

Fig. 9. The frequency deviation at area 2 under low RES penetration conditions.

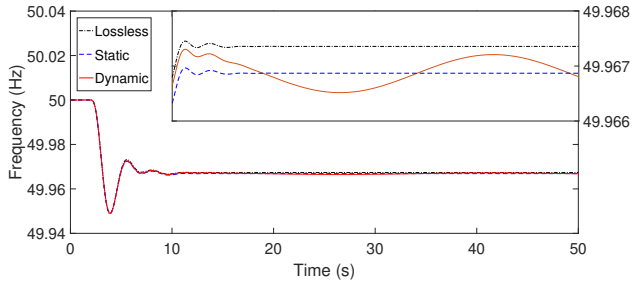

Fig. 10. The frequency deviation at area 2 under medium RES penetration conditions.

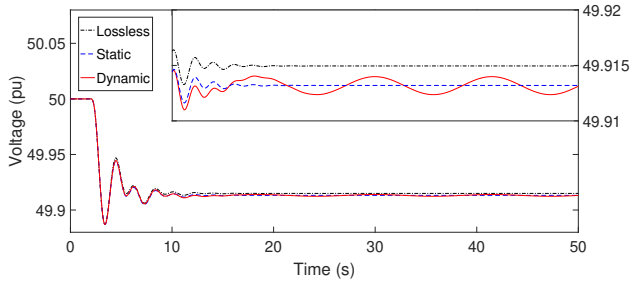

Fig. 11. The frequency deviation at area 2 under high RES penetration conditions.

(PSSs) are applied to generators or not. As we observe from both figures the proposed controller can significantly improve the voltage response of the system in both cases. We should mention that this improvement on both the voltage and the frequency was achieved without requiring all power system components (synchronous generators) to satisfy certain passivity conditions. Instead, the employment of such voltage droop controller at the loads provided additional damping to the system and thus increased its reliability and robustness during disturbances.

VIII. Conclusions

In this paper, we have presented a passivity-based framework for stability analysis and control design that allows more accurate modelling of both the network and the power system components while facilitating the derivation of completely decentralized stability results for the system. Throughout this work, it was also shown that the proposed framework could be exploited for the design of more accurate, distributed control schemes that can enhance the system's stability and

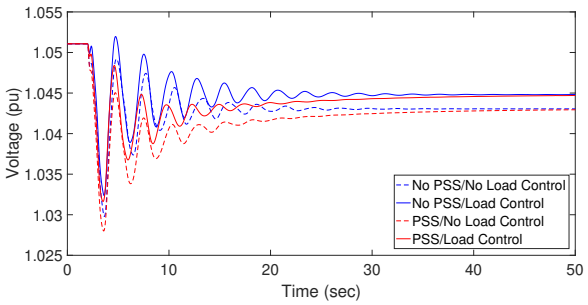

Fig. 12. The magnitude of the line current of a typical overhead $132kV$ transmission line.

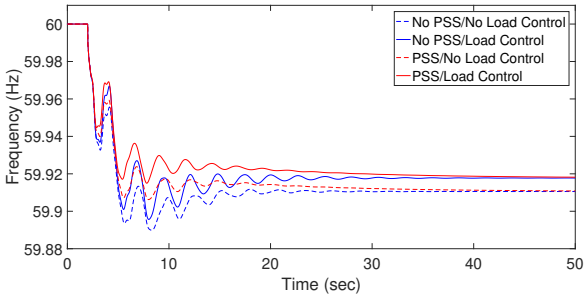

Fig. 13. The magnitude of the line current of a typical overhead $220kV$ transmission line.

robustness without requiring the implicit knowledge of the system. In particular, the proposed approach relied on the formulation of the network as a dynamical multi-variable system, which it was shown to be passive, even when the network's dynamic and lossy nature are taken into account. The passivity of the network was then exploited by introducing a broad class of bus dynamics to allow the incorporation of various power system components and certain decentralized, passivity conditions that can guarantee the asymptotic stability of the interconnected system. Moreover, we assessed the advantages and the opportunities offered by the proposed approach and demonstrated its applicability through the design of a voltage droop, load controller. Finally, we verified the significance of the adoption of such a multi-input/multi-output framework through several dynamic simulations on a simple test system and the IEEE 68 bus test system.

Appendix

Proof of Lemma 1: In order to prove that the dynamical system (11)-(12) is passive we use the following storage function:

$$\mathcal{V}^N(I_a, I_b) = \frac{1}{2}\begin{bmatrix} I_a^T & I_b^T \end{bmatrix}\begin{bmatrix} L & 0 \\ 0 & L \end{bmatrix}\begin{bmatrix} I_a \\ I_b \end{bmatrix}. \tag{28}$$

The derivative of the above storage function with respect to time is therefore given by:

$$\begin{aligned}\dot{\mathcal{V}}^N &= \begin{bmatrix} I_a^T & I_b^T \end{bmatrix} \begin{bmatrix} L & 0 \\ 0 & L \end{bmatrix} \begin{bmatrix} \dot{I}_a \\ \dot{I}_b \end{bmatrix} \\ &= \begin{bmatrix} I_a^T & I_b^T \end{bmatrix} \begin{bmatrix} -R & -\omega_s L \\ \omega_s L & -R \end{bmatrix} \begin{bmatrix} I_a \\ I_b \end{bmatrix} \\ &+ \begin{bmatrix} I_a^T & I_b^T \end{bmatrix} \begin{bmatrix} E^T & 0 \\ 0 & E^T \end{bmatrix} \begin{bmatrix} V_a \\ V_b \end{bmatrix} \\ &= -I_a^T R I_a - I_b^T R I_b + \begin{bmatrix} I_a^{nT} & I_b^{nT} \end{bmatrix} \begin{bmatrix} V_a \\ V_b \end{bmatrix}\end{aligned} \tag{29}$$

Since the network's resistance matrix R is a positive definite matrix, equation (29) satisfies $\dot{\mathcal{V}}^N \leq u^T y$ which completes the proof. □

Proof of Lemma 2: For the proof of the Lemma 2, we use the following storage function for the capacitance dynamics (18):

$$\mathcal{V}^C(V_a^c, V_b^c) = \frac{1}{2} \begin{bmatrix} V_a^{cT} & V_b^{cT} \end{bmatrix} \begin{bmatrix} \mathcal{C} & 0 \\ 0 & \mathcal{C} \end{bmatrix} \begin{bmatrix} V_a^c \\ V_b^c \end{bmatrix}. \tag{30}$$

The time derivative of the storage function (30) is therefore given by:

$$\begin{aligned}\dot{\mathcal{V}}^C &= \begin{bmatrix} V_a^{cT} & V_b^{cT} \end{bmatrix} \begin{bmatrix} \mathcal{C} & 0 \\ 0 & \mathcal{C} \end{bmatrix} \begin{bmatrix} \dot{V}_a^c \\ \dot{V}_b^c \end{bmatrix} \\ &= \begin{bmatrix} V_a^{cT} & V_b^{cT} \end{bmatrix} \begin{bmatrix} 0 & \omega_s \mathcal{C} \\ -\omega_s \mathcal{C} & 0 \end{bmatrix} \begin{bmatrix} V_a^c \\ V_b^c \end{bmatrix} \\ &+ \begin{bmatrix} V_a^{cT} & V_b^{cT} \end{bmatrix} \begin{bmatrix} I^{\mathcal{N}} & 0 \\ 0 & I^{\mathcal{N}} \end{bmatrix} \begin{bmatrix} -I_a^c \\ -I_b^c \end{bmatrix} \\ &= \begin{bmatrix} V_a^{cT} & V_b^{cT} \end{bmatrix} \begin{bmatrix} -I_a^c \\ -I_b^c \end{bmatrix}.\end{aligned} \tag{31}$$

From (31), we observe that $\dot{\mathcal{V}}^C = u^T y$ which implies that capacitance dynamics constitute a lossless system. □

Proof of Theorem 1: For the proof of Theorem 1 we employ the storage functions that follow from the passivity property of the branch, the capacitance and the bus dynamics to construct a candidate Lyapunov function for the interconnected system (20) - (21), (11) - (12) and (18). Stability will be then deduced using LaSalle's Invariance Principle [20].

We first consider the following candidate Lyapunov function for the interconnected system: (20)-(21), (11)-(12) and (18):

$$\mathcal{V}^S = \mathcal{V}^N + \mathcal{V}^C + \sum_{i=1}^{|\mathcal{N}|} \mathcal{V}_i. \tag{32}$$

Considering that Assumptions 1 - 4 hold, we then calculate the derivative of the above Lyapunov function with respect to time. We get:

$$\begin{aligned}\dot{\mathcal{V}}^S &= \dot{\mathcal{V}}^N + \dot{\mathcal{V}}^C + \sum_{i=1}^{|\mathcal{N}|} \dot{\mathcal{V}}_i \\ &= -(I_a - \hat{I}_a)^T R (I_a - \hat{I}_a) - (I_b - \hat{I}_b)^T R (I_b - \hat{I}_b) \\ &- \sum_{i=1}^{|\mathcal{N}|} \big(\psi_i(x - \hat{x}) + \phi_i(u - \hat{u}) + \rho_i(y - \hat{y}) \big)\end{aligned} \tag{33}$$

whenever $(\hat{I}_{a,i}^b,\ \hat{I}_{b,i}^b) \in U_i$ and $\hat{x}_i \in X$. Since the network's resistance matrix R and the functions $\psi_i(x - \hat{x})$, $\phi_i(u - \hat{u})$ and $\rho_i(y - \hat{y})$ are positive definite, the equation (33) becomes $\dot{\mathcal{V}}^S \leq 0$.

Subsequently, we use the LaSalle's theorem to prove the asymptotic convergence of the system's trajectories to the equilibrium point. According to Assumption 4, the candidate Lyapunov function $\mathcal{V}^S(x, I_a, I_b, V_a^c, V_b^c)$ has a strict local minimum at the equilibrium of the interconnected system $[\hat{x}^T\ \hat{I}_a^T\ \hat{I}_b^T\ \hat{V}_a^{cT}\ \hat{V}_b^{cT}]$. Thus, for a sufficiently small $\epsilon > 0$ there exists a compact positively invariant set $\Xi := \{\mathcal{V}^S(x, I_a, I_b, V_a^c, V_b^c) - \mathcal{V}^S(\hat{x}, \hat{I}_a, \hat{I}_b, \hat{V}_a^c, \hat{V}_b^c) \leq \epsilon,\ \hat{x} \in \Xi,\ \Xi\ connected\}$ that lies in the neighborhoods stated in Assumption 3. LaSalle's Invariance Principle can now be applied with the function $\mathcal{V}^S$ on the compact positively invariant set Ξ. This guarantees that all solutions of the interconnected system (20) - (21), (11) - (12) and (18) with initial conditions $[x(0)^T\ I_a(0)^T\ I_b(0)^T\ V_a^c(0)^T\ V_b^c(0)^T] \in \Xi$ converge to the largest invariant set within $\mathcal{D} := \Xi \cap \{x : \dot{\mathcal{V}}^S = 0\}$. From Assumptions 3 - 4, we get that the only invariant set in $\mathcal{D}$ is the equilibrium point $[\hat{x}^T\ \hat{I}_a^T\ \hat{I}_b^T\ \hat{V}_a^{cT}, \hat{V}_b^{cT}]$. Therefore, for any initial condition $[x(0)^T\ I_a(0)^T\ I_b(0)^T\ V_a^c(0)^T\ V_b^c(0)^T] \in \Xi$ we have convergence to the equilibrium point, which completes the proof. □

Proof of Proposition 1: For the proof of the Proposition 1 we consider the following storage function for the load dynamics (26) and (27):

$$\mathcal{V}_i^L = \frac{T_{c,i}}{2({k_{a,i}^c}^2 + {k_{b,i}^c}^2)} [I_{a,i}^{cl}\ I_{b,i}^{cl}] \begin{bmatrix} k_{a,i}^c & -k_{b,i}^c \\ k_{b,i}^c & k_{a,i}^c \end{bmatrix} \begin{bmatrix} I_{a,i}^{cl} \\ I_{b,i}^{cl} \end{bmatrix}. \tag{34}$$

The positive semidefiniteness of the above storage function follows here easily from the skew-symmetry of the matrix B_i^c and the fact that both the gain constants $k_{a,i}^c$ and $k_{b,i}^c$ are positive. The controllable load dynamics are therefore passive if the following inequality holds:

$$u_i^T y_i = [-I_{a,i}^b\ -I_{b,i}^b] \begin{bmatrix} V_{a,i}^b \\ V_{b,i}^b \end{bmatrix} \geq \dot{\mathcal{V}}_i^L \tag{35}$$

for all $i \in \mathcal{N}$. Considering that $\Delta V_{a,i} = V_{a,i}^b - V_{a,i}^{ref}$ and $\Delta V_{b,i} = V_{b,i}^b - V_{b,i}^{ref}$, we then calculate the derivative of the storage function (34) which is given by:

$$\begin{aligned}\dot{\mathcal{V}}_i^L =& \frac{-1}{({k_{a,i}^c}^2 + {k_{b,i}^c}^2)} [I_{a,i}^c\ I_{b,i}^c] \begin{bmatrix} k_{a,i}^c & -k_{b,i}^c \\ k_{b,i}^c & k_{a,i}^c \end{bmatrix} \begin{bmatrix} I_{a,i}^c \\ I_{b,i}^c \end{bmatrix} \\ &+ [I_{a,i}^c\ I_{b,i}^c] \begin{bmatrix} \Delta V_{a,i} \\ \Delta V_{b,i} \end{bmatrix} \\ =& \frac{-{k_{a,i}^c}^2}{({k_{a,i}^c}^2 + {k_{b,i}^c}^2)} ({I_{a,i}^{cl}}^2 + {I_{b,i}^{cl}}^2) \\ &- R_i^L ({I_{a,i}^l}^2 + {I_{b,i}^l}^2) + [-I_{a,i}^b\ -I_{b,i}^b] \begin{bmatrix} V_{a,i}^b \\ V_{b,i}^b \end{bmatrix}.\end{aligned} \tag{36}$$

Since $R_i^L,\ k_{a,i}^c,\ k_{b,i}^c \geq 0$, the equation (36) satisfies $\dot{\mathcal{V}}_i^L \leq u_i^T y_i$ and this completes the proof □.

REFERENCES

[1] H. Lund, *Renewable energy systems: a smart energy systems approach to the choice and modeling of 100% renewable solutions*. Academic Press, 2014.

[2] R. Teodorescu, M. Liserre, and P. Rodriguez, *Grid converters for photovoltaic and wind power systems*. J. Wiley & Sons, 2011, vol. 29.

[3] O. Sartor, T. Spencer, I. Bart, P. Julia, A. Gawlikowska-Fyk, K. Neuhoff, S. Ruester, A. Selei, A. Szpor, and B. Tóth, *EU's 2030 Climate and Energy Framework and Energy Security*. Climate Strategies., 2014.

[4] A. Ulbig, T. S. Borsche, and G. Andersson, "Impact of low rotational inertia on power system stability and operation," *IFAC Proceedings Volumes*, vol. 47, no. 3, pp. 7290–7297, 2014.

[5] F. Milano, F. Dörfler, G. Hug, D. J. Hill, and G. Verbič, "Foundations and challenges of low-inertia systems," in *2018 Power Systems Computation Conference (PSCC)*. IEEE, 2018, pp. 1–25.

[6] S.-F. Chou, X. Wang, and F. Blaabjerg, "Two-port network modeling and stability analysis of grid-connected current-controlled vscs," *IEEE Transactions on Power Electronics*, 2019.

[7] J. Schiffer, D. Zonetti, R. Ortega, A. M. Stanković, T. Sezi, and J. Raisch, "A survey on modeling of microgrids - from fundamental physics to phasors and voltage sources," *Automatica*, vol. 74, pp. 135–150, 2016.

[8] J. Schiffer, R. Ortega, A. Astolfi, J. Raisch, and T. Sezi, "Conditions for stability of droop-controlled inverter-based microgrids," *Automatica*, vol. 50, no. 10, pp. 2457–2469, 2014.

[9] J. Rocabert, A. Luna, F. Blaabjerg, and P. Rodriguez, "Control of power converters in ac microgrids," *IEEE transactions on power electronics*, vol. 27, no. 11, pp. 4734–4749, 2012.

[10] J. Schiffer, E. Fridman, and R. Ortega, "Stability of a class of delayed port-hamiltonian systems with application to droop-controlled microgrids," in *54th Conference on Decision and Control (CDC)*. IEEE, 2015.

[11] S. Trip, M. Bürger, and C. De Persis, "An internal model approach to (optimal) frequency regulation in power grids with time-varying voltages," *Automatica*, vol. 64, pp. 240–253, 2016.

[12] C. Zhao, U. Topcu, N. Li, and S. Low, "Design and stability of load-side primary frequency control in power systems," *IEEE Transactions on Automatic Control*, vol. 59, no. 5, pp. 1177–1189, 2014.

[13] A. Kasis, E. Devane, C. Spanias, and I. Lestas, "Primary frequency regulation with load-side participation—part i: Stability and optimality," *IEEE Trans. on Power Systems*, vol. 32, no. 5, pp. 3505–3518, 2017.

[14] S. Trip and C. De Persis, "Distributed optimal load frequency control with non-passive dynamics," *IEEE Transactions on Control of Network Systems*, vol. 5, no. 3, pp. 1232–1244, 2017.

[15] T. Stegink, C. De Persis, and A. van der Schaft, "A unifying energy-based approach to stability of power grids with market dynamics," *IEEE Transactions on Automatic Control*, vol. 62, no. 6, pp. 2612–2622, 2017.

[16] C. Spanias and I. Lestas, "A system reference frame approach for stability analysis and control of power grids," *IEEE Transactions on Power Systems*, vol. 34, no. 2, pp. 1105–1115, 2019.

[17] J. Machowski, J. Bialek, and J. Bumby, *Power system dynamics: stability and control*. J. Wiley & Sons, 2011.

[18] ENTSO-E, "Commission regulation (eu) 2016/631 of 14 april 2016 establishing a network code on requirements for grid connection of generators," *OJ*, vol. L 112, pp. 1–68, 2016-04-27.

[19] N. Pogaku, M. Prodanovic, and T. C. Green, "Modeling, analysis and testing of autonomous operation of an inverter-based microgrid," *IEEE Transactions on power electronics*, vol. 22, no. 2, pp. 613–625, 2007.

[20] H. K. Khalil, *Nonlinear Systems*, 3rd ed. Prentice Hall, 2002.

[21] J. Bao, P. L. Lee, and B. E. Ydstie, "Process control: the passive systems approach," Ph.D. dissertation, Springer-Verlag, 2007.

[22] S. Boyd, L. El Ghaoui, E. Feron, and V. Balakrishnan, *Linear matrix inequalities in system and control theory*. Siam, 1994, vol. 15.

[23] C. Spanias, P. Aristidou, and M. Michaelides, "A dynamical multi-input/multi-output network formulation for stability analysis in AC microgrids," in *Innovative Smart Grid Technologies (ISGT) Europe*, 2019, pp. 1–5.

[24] J. Watson, Y. Ojo, I. Lestas, and C. Spanias, "Stability of power networks with grid-forming converters," in *2019 IEEE Milan PowerTech*. IEEE, 2019, pp. 1–6.

[25] P. Aristidou and G. Hug, "Accelerating the computation of critical eigenvalues with parallel computing techniques," in *2016 Power Systems Computation Conference (PSCC)*. IEEE, 2016, pp. 1–8.

[26] C. Spanias, P. Aristidou, M. Michaelides, and I. Lestas, "Power system stability enhancement through the optimal, passivity-based, placement of svcs," in *2018 Power Systems Computation Conference (PSCC)*. IEEE, 2018, pp. 1–7.

[27] C. Spanias, P. Aristidou, and M. Michaelides, "Demand-side Volt/Var/Watt regulation for effectivevoltage control in distribution grids," in *Innovative Smart Grid Technologies (ISGT) Europe*, 2019, pp. 1–5.

[28] G. Rogers, *Power system oscillations*. Springer Science & Business Media, 2012.